

## Use of Building Automation System Trend Data for Inputs Generation in Bottom-Up Simulation Calibration

Nicholas F. Zibin

*Center for Zero Energy Building  
Studies*

*Department of Building, Civil, and  
Environmental Engineering  
Concordia University, Montreal,  
Canada*

Radu G. Zmeureanu

*Center for Zero Energy Building  
Studies*

*Department of Building, Civil, and  
Environmental Engineering  
Concordia University, Montreal,  
Canada*

James A. Love

*Faculty of Environmental Design  
University of Calgary, Canada*

### ABSTRACT

Ongoing commissioning based on calibrated energy models is one of the most promising means to improve the energy performance of existing buildings. The bottom-up calibration approach starts the calibration on a zone level before sequentially calibrating the system, plant, and whole-building level models. The hypothesis is that bottom-up calibration can create more reliable and accurate models than those created with existing approaches. The number of candidate measurement points to be considered for analysis and use in simulation is very large. This paper explores automating the process of generating inputs from Building Automation System (BAS) trend data for use in building simulation software. A proof-of-concept prototype called the Automatic Assisted Calibration System (AACCS) was created which generated multiple eQUEST inputs from BAS trend data obtained from a case study building.

### BACKGROUND

Commercial and institutional buildings are responsible for 14% of total energy use and 13% of greenhouse gas emissions in Canada (NRCAN 2009). The prevalence of older buildings among this stock means they will be key in reducing energy use and related emissions in this sector. Continuous evaluation of building performance is a management tool that could reduce energy use and associated negative environmental effects.

Building systems are often poorly maintained and improperly controlled, resulting in an estimated 15% to 30% waste of energy (Katipamula and Brambley 2005). Commissioning helps reduce this energy waste by assuring that the energy and environmental control performance of a building meets or exceeds the design intent, after construction is complete. As a building operates, equipment degrades, faults occur, requirements change and

operators change control settings for a variety of reasons, which may improve or impair energy and/or environmental control performance. To achieve an optimal level of energy and environmental control performance, ongoing commissioning or existing building commissioning monitors on a continuing basis the air-handling units (AHUs) and the heating and cooling plants within a building (Monfet and Zmeureanu 2012). Within this approach, the use of calibrated building energy models can be a useful building performance management tool (Costa et al. 2013) to identify energy efficiency measures, create benchmarks for operation, and estimate future performance under new operating conditions.

This paper proposes a system to automate the generation of inputs from Building Automation System (BAS) trend data for use in calibrating building energy models using a bottom-up approach, where an analyst sequentially calibrates the zone level model before the system, plant, and whole-building level models. The hypothesis is that bottom-up calibration can create more accurate and reliable models than those created with existing approaches. The number of candidate measurement points required to execute bottom-up calibration is very large. The proposed system could reduce the time and effort required to analyse large sets of trend data for use in calibrating building energy models. In this paper inputs are information entered into building simulation software and trend data is ongoing measurements recorded in a BAS.

### LITERATURE REVIEW

A calibrated building energy model generates estimates that match the measured energy use of an existing building with acceptable accuracy. In calibrating models, it is common to use a top-down approach, where an analyst tunes certain model inputs, either heuristically or based on optimization techniques, until the simulation results fit whole building utility data or other measurements with an acceptable error. The heuristic approaches, described in Reddy's literature review (2006), generally include

three steps: (1) creating a “first cut” simulation model, (2) comparing the simulation estimate with the metered energy use, and (3) using experience to iteratively modify the model inputs to improve the fit of the simulation estimate to measured use. Optimization methods have also been proposed where inputs are estimated from the minimization of the difference between the measured monthly energy use and the simulation results (Liu and Henze 2005; Sun and Reddy 2006; Reddy et al. 2007).

An existing building simulation model can be calibrated at various levels of detail: the whole-building, plant, system, or zone level models (Figure 1). A similar classification system was proposed by Maile et al. (2012). Previous literature focused on calibrating at the whole-building level where it is unknown whether offsetting errors in the model could exist at various levels such as thermal zones and HVAC systems and plants. It is also unknown whether key model zone, system, and plant performance have been characterized with sufficient accuracy. More recent publications deal with the calibration on a system and plant level. Tian and Love (2009) calibrated a building on a plant level using monthly metered thermal energy for heating and cooling, and electricity for lighting/equipment. Monfet et al. (2009) calibrated a building at the system level using the thermal loads of an institutional building and the supply air flow rate of the air-handling unit (AHU).

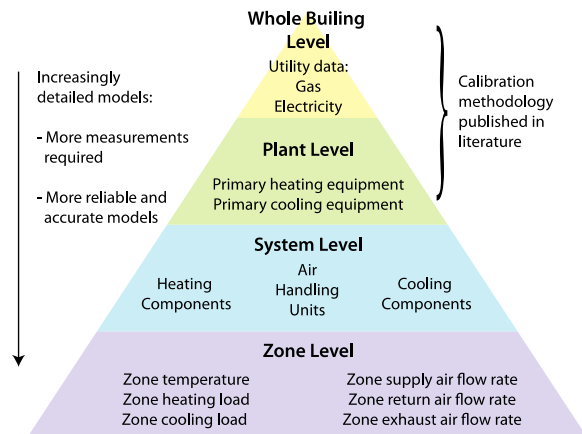


Figure 1. Classification of calibration methods

## METHOD

The common top-down approach uses deductive reasoning, assuming that if the whole-building or plant level model is calibrated, then the system and zone level models are likely to be calibrated. The bottom-up calibration procedure proposed here uses inductive reasoning in the form of evidence from

measurements addressing the zone level model first; zone temperatures, supply/return air flow rates, and zone cooling/heating loads etc., are calibrated depending on the available measurements. This is followed by the calibration of the system level model (eg. AHU supply, return, and exhaust air flow rates, and supply/return air temperature, heating and cooling coil capacities, fan performance, thermofluid flow rates, etc.). The plant level is addressed next, where a building’s heating and cooling primary equipment are calibrated. The final step is the calibration at the whole-building level using utility data. A more accurate and reliable representation of actual building performance is achieved if all the level models are calibrated.

The two main reasons building simulation models are often calibrated on a whole-building or plant level are (1) monthly utility energy use for gas and electricity are the most available measurements and (2) the time and effort required to calibrate at the zone or system level (if the corresponding measurements are available) is substantially greater when compared to calibrating on a whole-building level. Model calibration methods have been applied to simplified models (Liu, M., and G. Liu 2011; Heo et al. 2012) and to detailed simulation models created with software such as eQUEST and EnergyPlus (Monfet et al. 2009). Heo et al. (2012) showed that simplified models could be as accurate as detailed models at the whole building level. However, Raferty et al. (2011) argued that simplified models could not represent energy efficiency measures at the zone, system, and plant levels.

To the authors’ knowledge, there are no publications discussing the extraction of inputs from BAS trend data to calibrate simulation models. Pang et. al (2012) used trend data to calibrate a building energy model but did not discuss how their inputs were generated. There is currently little use of trend data in calibrating building simulation models. This is due to the difficulty in achieving a calibrated model and the, often large, difference between measured energy use and simulation estimates. Typical BAS trend data includes temperature, humidity, and air flow rates; rarely are thermofluid flow rates and sub-hourly electric demand available. This paper is a contribution in combining measured data and building simulation.

The system, shown in Figure 2, is called the Automatic Assisted Calibration System (AACS). The AACS assists an analyst by automating the interaction between trend data analysis and the generation of inputs for use in building simulation

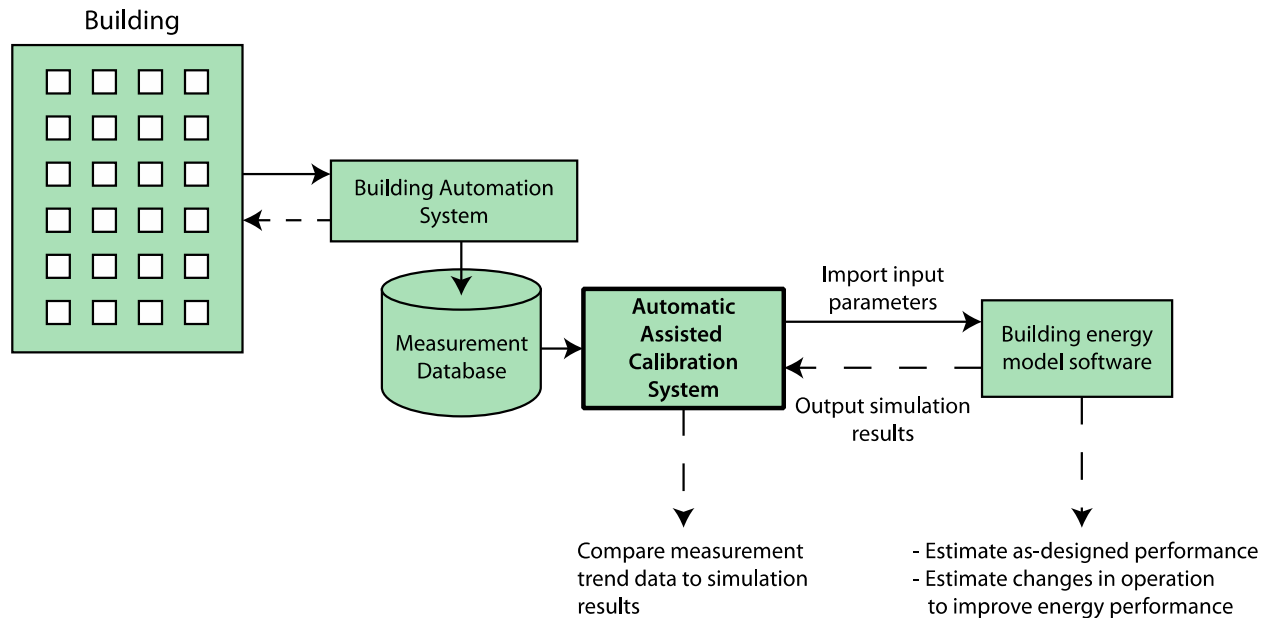


Figure 2. Assisted Automatic Calibration System schematic

software. Ideally, the AACS generates relevant inputs during each of the cooling, heating, and shoulder seasons. It does not automatically produce a calibrated model but assists in the calibration process. This differs from programs that automatically create a calibrated model by tuning inputs based on an optimization approach such as SIMEB (Millette et al. 2011). The AACS is connected to a database created from the weekly export of a comma separated value (CSV) file produced by the BAS. The trend data is processed into inputs that are directly entered into programs such as eQUEST and EnergyPlus. The building simulation software exports its results to the AACS, where the simulation results are compared to the measured data using statistical techniques.

The proposed AACS approach was used for a calibration case study of a new research centre, recently completed on the Loyola campus of Concordia University in Montreal. The next section presents the building and HVAC systems, while the following section presents the available BAS trend data, and the generation of inputs for eQUEST. eQUEST was chosen as the simulation software because, at the time of writing, Natural Resources Canada is developing a version for use in Canada (Can-QUEST).

## BUILDING DESCRIPTION

The Research Centre for Structural and Functional Genomics, known as the Genome Building (Figure 3), was completed in spring, 2012.

It has a floor area of 5200 m<sup>2</sup> (56,000 ft<sup>2</sup>), consisting of 5 levels, including a basement and a mechanical penthouse. The building has an orientation of approximately 60° west of north and a window-to-wall ratio of 33%. The building houses laboratories, offices, conference rooms, and a small data centre, located in the basement. The laboratory equipment includes environmental chambers, ventilation hoods, and other equipment required for biological experiments. The BAS software is Siemens APOGEE. The information presented in this section was extracted from construction documents. The opaque façade and roof have nominal U-values of 0.27 (0.048) and 0.19 (0.033) W/m<sup>2</sup>·K (Btu/h·ft<sup>2</sup>·°F), respectively.

### Air Distribution System

The Genome Building has a variable-air-volume (VAV) system. Two identical air-handling units (AHUs), connected in parallel, with a total supply air flow capacity of 42,500 L/s (90,000 cfm) and return capacity of 14,200 L/s (30,000 cfm), are located in the mechanical penthouse. Air is returned via plenums ducts in two risers. Air is drawn from ventilation hoods, laboratories, and restrooms through two parallel exhaust fans with a capacity of 33,000 L/s (70,000 cfm). The air within the AHUs are conditioned using run-around sensible heat recovery preheating coils, heating coils, cooling coils, and steam humidification.



Figure 3. The Genome Building located on Concordia University Loyola Campus in Montreal, Canada

#### Heat recovery preheat/precool system.

Exhaust air is passed through heat recovery glycol coils (SR1) (Figure 4), which can preheat or precool the outdoor air entering the AHUs. When  $T_{oa}$  is less than  $8\text{ }^{\circ}\text{C}$  ( $46\text{ }^{\circ}\text{F}$ ) or greater than  $28\text{ }^{\circ}\text{C}$  ( $82\text{ }^{\circ}\text{F}$ ) the pump (P03) runs continuously at a glycol flow rate of  $11.7\text{ L/s}$  ( $185\text{ US gm}$ ). A three way valve is used to maintain the temperature of the glycol returning to the recovery coil (SR1) ( $T_{glcr}$ ), at  $4\text{ }^{\circ}\text{C}$  ( $39\text{ }^{\circ}\text{F}$ ) or higher to prevent frosting in the AHUs.

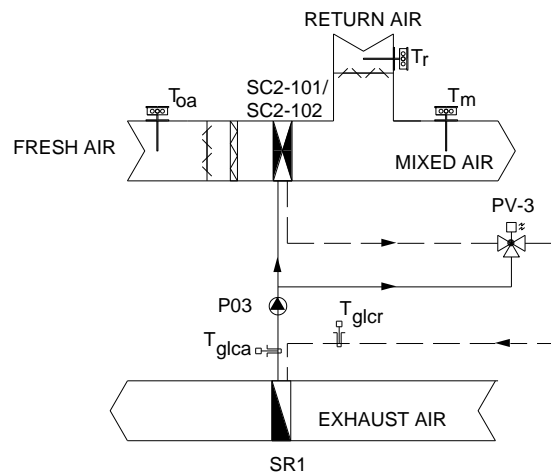


Figure 4. Simplified run-around heat recovery preheat system in the AHUs

#### Heating Plant

The Loyola Campus central plant serves the building, providing hot water and steam, which are used to heat and humidify supply air. The centrally-supplied hot water is passed through: (1) two parallel heat exchangers that provide heat to the heating coils in the AHUs via a glycol loop and (2) a hot water loop for VAV reheat of the supply air entering the rooms. The heating coil pump operates with a

variable frequency drive with a  $5.8\text{ L/s}$  ( $92\text{ US gm}$ ) design capacity.

#### Cooling Plant

The campus chilled water loop normally supplies chilled water to the building. When the cooling demand is large, a  $1760\text{ kW}$  ( $500\text{ ton}$ ) chiller located in the mechanical penthouse provides additional chilled water.

### **ANALYSIS AND INPUTS GENERATION**

This section presents the analysis of trend data collected and how they were processed into inputs for the eQUEST model. The analysis is presented starting on a zone level, followed by the system level. All trend data was recorded under real operating conditions.

#### Analysis of Trend Data

The available BAS trend data (Table 1), used in this analysis, were recorded as ongoing measurements every 15 min. All measured data is presented using hourly averaged values calculated from the 15 min data. Considerable time is required to manually analyze and extract inputs from 248 trend data points, which demonstrates the need for an AACS. Data monitoring started June 2012 when construction was complete. This analysis was based on data collected during the heating season from January 7th to March 31st 2013, unless otherwise stated. January 7th was chosen because this was the first day that the building was in use after winter holidays. The database of trend data was imported into MATLAB where a proof-of-concept prototype AACS was created.

The first step to test the AACS proof-of-concept was to manually organize the trend data based on a spatial and thermal hierarchy similar to the one proposed by Maile et al. (2012), as discussed in the literature review. Once the trend data was organized, the analyst selected the time period for analysis and the AACS generated inputs based on the methods used in the next sections. All data that appeared erroneous, based on inspection and judgement, were removed.

#### Generation of Zone Level Inputs

A total of 17 thermal zones were defined based on space function, proximity to the exterior, and orientation. The basement and mechanical penthouse

Table 1. Available BAS trend data

Trend Data	No. of sensors	Sensor accuracy	Unit
<b>Ambient</b>			
Outside air temperature	1	± 0.3	°C
Outside air humidity	1	± 2%	%
<b>Zone Level</b>			
Room air temperature	95	± 0.3	°C
Zone perimeter supply air temp.	2	± 0.3	°C
Fume hood exhaust rate	4	± 5%	L/s
Room air supply flow rate	105	± 5%	L/s
Zone return/exhaust flow rate	18	± 5%	L/s
<b>System Level</b>			
<b>AHUs</b>			
Supply air temperature	2	± 0.3	°C
Mixed air temperature	2	± 0.3	°C
Return air temperature	2	± 0.3	°C
Total return air flow rate	2	± 5%	L/s
Total supply air flow rate	4	± 5%	L/s
Supply air humidity	2	± 2%	%
Return air humidity	2	± 2%	%
<b>Heat Recovery</b>			
Glycol recovery supply temp.	1	± 0.3	°C
Glycol recovery return temp.	1	± 0.3	°C
<b>Heating Coils</b>			
Glycol supply temperature	2	± 0.3	°C
Glycol return temperature	2	± 0.3	°C
<b>Total</b>	248		

were not modelled. The zone trend data included: (1) room temperatures, (2) room supply air flow rates, (3) zone return air and exhaust flow rates, and (4) fume hood exhaust flow rates.

The AACS generated the temperature set point schedule for input into eQUEST (HEAT-TEMP-SCH) for each zone. First, zone hourly average temperatures were calculated by averaging temperature trend data for all rooms located in a zone. A single average zone temperature for a day and night schedule on weekdays and an average daily zone temperature on weekends were created (Table 2). The day period during weekdays is defined as

07:00 to 23:00 based on trend data of the minimum and maximum zone supply air flow.

The AACS calculated supply air flow rates for each zone from the summation of the VAV terminal supply air flow rate trend data in the zone. The AACS generated the zone design air flow rate (ASSIGNED-FLOW) as the maximum measured zone supply air flow rate. The eQUEST hot deck ratio of minimum to maximum zone supply air flow rate (HMIN-FLOW-RATIO) for each zone was also generated in the AACS as the ratio of the measured minimum to maximum supply air flow rate in the zone. The results for the inputs generated at zone level are summarized in Table 2.

#### Generation of System Level Inputs

The trend data is discussed in terms of the AHUs, run-around heat recovery preheat, and heating components.

#### Air handling units.

The temperatures and air flow rates measured within the AHUs were also used in the AACS to generate inputs. It is common to use set points specified in the design specifications or as-built commissioning documents as inputs, however analysis of data from the system level can provide insight into actual system performance. For example, the measured supply air temperature from the AHUs was plotted over the controlled reset of supply air temperature set point as a function of the outdoor air temperature ( $T_{oa}$ ) (Figure 5). When the outdoor air temperature was below -10 °C (14 °F), the system operated near the desired set point. The supply air was overcooled when  $T_{oa}$  was between 10 °C (50 °F) and -10 °C (14 °F). The temperature reset schedule generated by the AACS should therefore reflect regular operating conditions.

The maximum measured supply air flow rate in the AHUs was calculated in the AACS to generate the design supply air flow rate (SUPPLY-FLOW). The ratio of measured minimum to maximum supply air flow rate was calculated in the AACS to generate the heating minimum flow ratio (HMIN-FLOW-RATIO). The design return air flow rate in eQUEST (RETURN-FLOW) was calculated in the AACS as the maximum measured return air flow rate. The AACS also calculated the maximum and minimum return air relative humidity for input into eQUEST's humidity control (MIN- and MAX-HUMIDITY).

Table 2. Zone level inputs generated from trend data

Zone	Zone Temperature Average (°C)			Supply Air Flow	
	Weekday		Weekend	Max. (L/s)	Min Flow ratio
	Day	Night			
<b>Z1-S</b>	21.2	19.4	20.2	956.5	0.00
<b>Z1-NE</b>	23.3	22.3	22.6	757.4	0.22
<b>Z1-NW</b>	20.6	20.2	20.2	1430.8	0.46
<b>Z1-CORR</b>	21.7	21.5	21.6	578.1	0.61
<b>Z1-CONF</b>	23.9	23.9	23.7	546.5	0.46
<b>Z2-SE</b>	23.1	22.1	22.7	1389.7	0.27
<b>Z2-E</b>	22.3	22.2	22.2	2488.8	0.41
<b>Z2-INT</b>	23.0	22.9	22.9	504.9	0.51
<b>Z2-NE</b>	22.5	21.3	20.9	1836.6	0.47
<b>Z2-S</b>	22.4	22.4	22.5	634.7	0.72
<b>Z2-W</b>	22.2	22.4	22.3	276.5	0.00
<b>Z3-SE</b>	22.7	21.3	22.1	1520.9	0.29
<b>Z3-E</b>	22.8	22.6	22.7	2479.8	0.71
<b>Z3-INT</b>	23.5	23.4	23.4	462.9	0.35
<b>Z3-NE</b>	21.6	20.8	20.2	1527.1	0.41
<b>Z3-S</b>	22.3	22.4	22.3	874.0	0.25
<b>Z3-W</b>	22.3	22.5	22.3	292.1	0.25

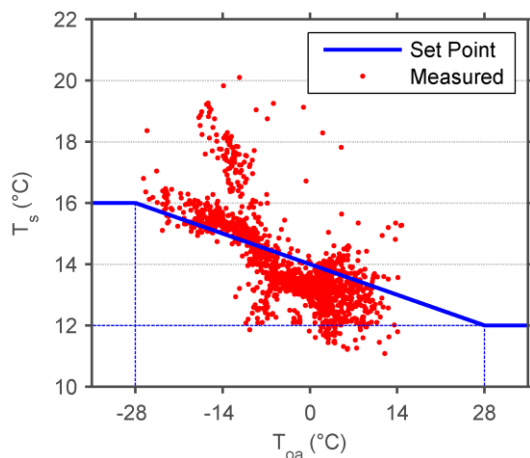


Figure 5. Comparison of the measured and reset supply air temperature BAS set point

#### Run-around heat recovery preheat coils.

Heat is recovered from the exhaust air to preheat the outdoor air (Figure 4). The damper positions in the AHUs were not recorded, so the ratio of outdoor to supply air flow ( $\alpha$ ) was unknown. Using the

available trend data,  $\alpha$  could be estimated (eq. 1) along with other inputs needed to simulate the run-around heat recovery preheat coils. As in Moser (2013),  $\alpha$  was calculated as the slope of the curve fit when zero preheating of the outdoor air occurred (Figure 6). There were three distinct operating conditions that are summarized in Table 3 and shown as regions I, II, and III in Figure 6. The calculated air temperature, in the AHU, after the run-around heat recovery preheat coils ( $T_{PH}$ ) could be used to estimate  $\alpha$  using eq. 2 for regions II and III.

$$\alpha_I = \frac{\dot{m}_{oa}}{\dot{m}_s} = \frac{T_m - T_r}{T_{oa} - T_r} \quad (1)$$

$$\alpha_{II,III} = \frac{\dot{m}_{oa}}{\dot{m}_s} = \frac{T_m - T_r}{T_{PH} - T_r} \quad (2)$$

where:  $T_{PH}$  is the air temperature after the run-around heat recovery preheat coils  
 $T_r$  is the return air temperature in the AHU



Table 3. Run-around heat recovery preheat loop operation summary

Region	Date	Description
I	Nov 1 <sup>st</sup> – Dec 22 <sup>nd</sup> 2012.	When $T_{oa}$ is less than 8 °C (46 °F) the run-around heat recovery coils should operate to preheat the outdoor air. However, pump P03 did not function so no preheating occurred.
II	Jan 7 <sup>th</sup> – Mar 31 <sup>st</sup> 2013.	Pump P03 operated at a constant flow rate and preheated the outdoor air to a constant $T_{PH}$ as $T_{oa}$ got colder.
III	Jan 7 <sup>th</sup> – Mar 31 <sup>st</sup> 2013.	Pump P03 continued to operate and valve PV-3 opened to maintain the temperature entering the recovery coil (SR1) ( $T_{glcr}$ ) to 4 °C (39 °F). The amount of energy transferred to preheat the outdoor air was limited causing $T_{PH}$ to decrease as $T_{oa}$ gets colder.

The run-around heat recovery preheat loop was activated when  $T_{oa}$  was less than 8°C (corresponding to -14°C on the  $x$ -axis of Figure 6) according to the control sequence as programmed in the BAS. Once  $T_{PH}$  can be estimated in the AACS using the linear regressions in regions I, II, and III, the minimum  $\alpha$  could be calculated using eq. 2 for input into

eQUEST as the minimum outside air ratio (MIN-OUTSIDE-AIR). On a side note  $T_r$ , which influences  $\alpha$ , was measured at a relatively constant temperature with mean values of 21.5 °C (71 °F), 22.2 °C (72 °F), and 22.5 °C (73 °F) with an uncertainty of 0.4 °C (0.7 °F) in regions I, II, and III, respectively. Generating inputs in the AACS from the heat recovery preheat loop is being investigated further.

#### Heating coils.

The temperature of glycol entering the heating coils ( $T_{hwa}$ ) in the AHUs follows a controlled reset temperature set point, as a function of  $T_{oa}$  (Figure 7). The trend data shows that the reset profile was followed, however, with a higher glycol supply temperature. The corrected reset profile was estimated manually from the  $T_{hwa}$  trend data using linear regression (Table 4), because, at the time of writing, the AACS could not automatically calculate temperature reset schedules.

The glycol mass flow rate ( $\dot{m}_{glc}$ ) in the heating coils was not measured. However, the AACS could calculate  $\dot{m}_{glc}$  using eq. 3. The hot deck temperature ( $T_{HT}$ ) was not measured, but was estimated by subtracting the temperature rise across the supply fan ( $\Delta T_{fan}$ ) from the supply air temperature (measured after the fan). The temperature rise across the supply fan in eQUEST (SUPPLY-DELTA-T) is another input that was calculated in the AACS. During hours with zero heating or cooling (automatically found in the AACS)  $\Delta T_{fan}$  was calculated as an average of 1.8

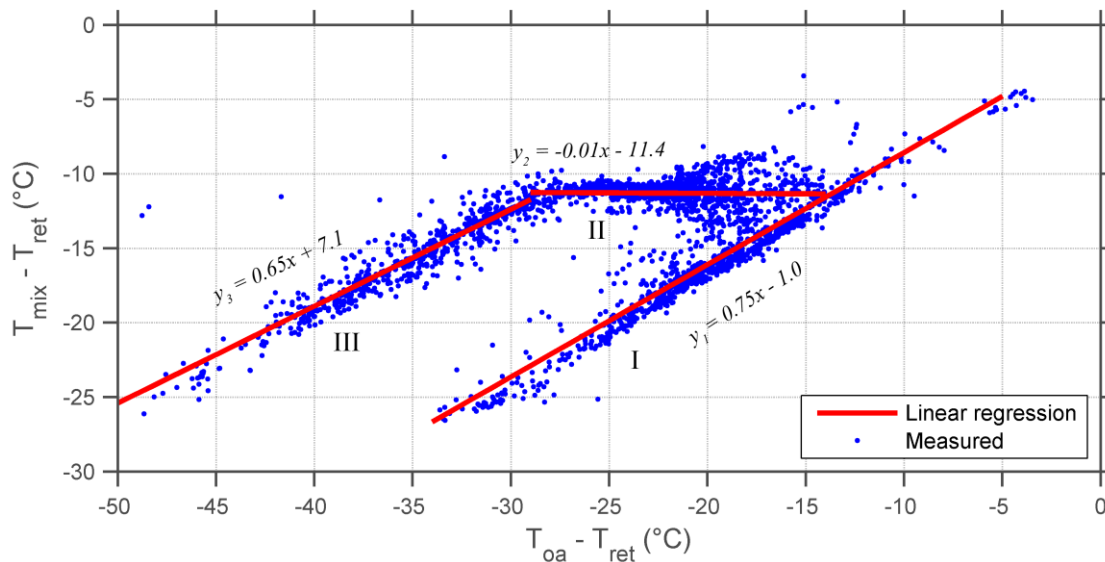


Figure 6. Economizer and run-around heat recovery preheat coil analysis, similar to Moser (2013)

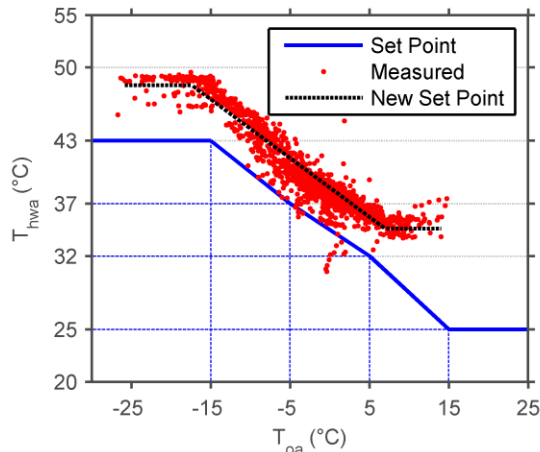


Figure 7. Comparison of the measured and hot glycol reset temperature BAS set point

°C (3.2 °F) with an uncertainty of 0.4°C (0.7 °F) by subtracting the mixed air temperature from the supply air temperature in the AHU. eQUEST's SUPPLY-DELTA-T default value for VAV fans is 1.9 °C (3.4 °F).

$$q_{heat} = \dot{m}_s c_{p_{air}} (T_{HT} - T_m) = \dot{m}_{glc} c_{p_{glc}} (T_{hwa} - T_{hwr}) \quad (3)$$

where:  $T_{hwa}$  is the glycol temperature arriving at the heating coils  
 $T_{hwr}$  is the glycol temperature returning from the heating coils  
 $T_{HT}$  is the hot deck temperature;

$$T_{HT} = T_s - \Delta T_{fan}$$

$T_m$  is the mixed air temperature in the AHU  
 $\Delta T_{fan}$  is the temperature rise across the fans

Table 4. Measured hot glycol temperature reset

Hot glycol reset input: HEAT-RESET-SCH	Temperature °C (°F)
SUPPLY-HI	48.3 (119)
OUTSIDE-LO	-17.4 (0.7)
SUPPLY-LO	35 (95)
OUTSIDE-HI	7 (45)

The estimated mass flow rate of glycol versus outdoor air temperature is plotted in Figure 8. The maximum glycol flow rate was estimated in the AACS to generate the pump flow rate in eQUEST (FLOW). The maximum glycol temperature difference across the heating coils was calculated in

the AACS for input into eQUEST as the design temperature change through the heating coil (HW-COIL-DT). The capacity of the heating coils (HEATING-CAPACITY) was generated in the AACS as the maximum  $q_{heat}$  value calculated using eq. 3.

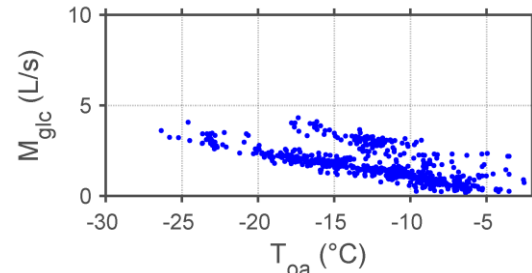


Figure 8. Estimated heating coil glycol flow rate

The results for the inputs generated in the AACS at the system level are summarized in Table 5. At the time of writing, no total plant or whole-building trend data were available.

## FUTURE WORK

The next step in this research is to calibrate simulations of the Genome Building using information from as-built drawings and the inputs generated in the AACS. For further development of an AACS, issues with faults and data quality must be addressed. The AACS could also be improved by automatically estimating temperature reset, lighting, and occupancy schedules etc., if the required sensors were available. Further investigation is required to fully extract all the inputs from the run-around heat recovery preheat system and the economizer. The BAS system records trend data for the supply and return chilled water temperatures and supply and return condenser water temperatures. Cooling system inputs could be generated using this trend data if the cooling season was analysed.

Even with the large number of inputs that could be extracted from a BAS, unknown inputs remain. Using supplementary loggers such as electricity and flow meters could generate some remaining inputs. In commercial and institutional buildings, some influential inputs, such as infiltration and effective wall U-value, are very difficult to measure.

## CONCLUSION

An Automatic Assisted Calibration System (AACS) was proposed to automate the process of analysing BAS trend data to generate inputs for building simulation. Multiple inputs were generated



Table 5. System level inputs generated from BAS measurements

System	Description	eQUEST Inputs	Value	
AHUs	Maximum supply air flow	SUPPLY-FLOW	33,800	L/s
	Minimum supply air flow ratio	HMIN-FLOW-RATIO	0.50	-
	Return design flow rate	RETURN-FLOW	11,700	L/s
	$\Delta T_{fan}$	SUPPLY-DELTA-T	1.8	°C
	Maximum return relative humidity	MAX-HUMIDITY	30.6	%
	Minimum return relative humidity	MIN-HUMIDITY	29.3	%
Heating coils	Glycol $\Delta T$	HW-COIL-DT	37.4	°C
	Maximum glycol flow rate	FLOW	4.3	L/s
	Heating coil capacity	HEATING-CAPACITY	510	kW

on a zone and system level from trend data in an existing building to verify the proof-of-concept. The generated eQUEST inputs could be used as the starting point for creating a calibrated model using a bottom-up approach. The hypothesis is that bottom-up calibration can create more reliable and accurate models than those created with the top-down approach.

Integrating or coupling an AACS with building simulation software could reduce the time and effort required for bottom-up calibration. In the future the AACS could automatically enter inputs calculated from BAS trend data into building simulation software. The automatic generation of inputs from BAS trend data could become a powerful tool in creating calibrated building simulation models.

#### ACKNOWLEDGEMENTS

The authors acknowledge financial support provided by the Faculty of Engineering and Computer Science (Concordia University) and the NSERC Smart Net-Zero Energy Buildings Strategic Research Network. The first author acknowledges the ASHRAE Graduate Student Grant-In-Aid Award (2013-2014) and the NSERC Postgraduate (Master's) Scholarship.

#### REFERENCES

- Costa, A., M.M. Keane, J.I. Torrens, and E. Curry. 2013. Building operation and energy performance: Monitoring, analysis and optimisation toolkit. *Applied Energy* 101:310–16.
- Heo, Y., R. Choudhary, and G. A. Augenbroe. 2012. Calibration of building energy models for retrofit analysis under uncertainty. *Energy and Buildings* 47:550-560.
- Katipamula, S., and M. R. Brambley. 2005. Review Article: Methods for Fault Detection, Diagnostics, and Prognostics for Buildings Systems – A Review, Part I. *HVAC&R Research* 11(1):3–25.
- Liu, S., and G.P. Henze. 2005. Calibration of building models for supervisory control of commercial buildings. *Proceedings of the IBPSA Building Simulation Conference, Montreal, Canada*, 641-48.
- Liu, G., and M. Liu. 2011. Applications of a Simplified Model Calibration Procedure for Commonly Used HVAC Systems. *ASHRAE Transactions* 117(1):835–46.
- Maile, T., V. Bazjanac, and M. Fischer. 2012. A method to compare simulated and measured data to assess building energy performance. *Building and Environment* 56:241-51.
- Millette, J., S. Sansregret, and A. Daoud. 2011. SIMEB: Simplified interface to DOE2 and EnergyPlus – A user's perspective – Case study of an existing building. *Proceedings of the IBPSA Building Simulation Conference, Sydney, Australia*, 2349-55.
- Monfet, D., R. Zmeureanu, R. Charneux, and N. Lemire. 2009. Calibration of a Building Energy Model Using Measured Data. *ASHRAE Transaction* 115(1):348–59.
- Moser, D.E. 2013. Commissioning Existing Airside Economizer Systems. *ASHRAE Journal* 55(3):34-44.

- NRCan. 2009. Energy Efficiency Trends in Canada 1990 to 2009. Natural Resources Canada, Canada.
- Pang, X., M. Wetter, P. Bhattacharya, and P. Haves. (2012). A framework for simulation-based real-time whole building performance assessment. *Building and Environment*, 54:100-08.
- Raferty, P., M. Keane, J. O'Donnell. 2011. Calibrating whole building energy models: An evidence-based methodology. *Energy and Buildings* 43:2356-64.
- Reddy, T.A. 2006. Literature Review on Calibration of Building Energy Simulation Programs: Uses, Problems, Procedures, Uncertainty, and Tools. *ASHRAE Transactions* 112(1):226-40.
- Reddy, T.A., I. Maor, and C. Panjapornpon. 2007. Calibrating Detailed Building Energy Simulation Programs with Measured Data – Part 1: General Methodology (RP-1051). *HVAC&R Research* 13(2):221-41.
- Sun, J., and T.A. Reddy. 2006. Calibration of Building Energy Simulation Programs Using the Analytical Optimization Approach (RP-1051). *HVAC&R Research* 12(1):177-96.
- Tian, Z., and J.A. Love. 2009. Energy performance optimization of radiant slab cooling using building simulation and field measurements. *Energy and Buildings* 41:320-30.